

Multilayered chromium/chromium nitride coatings for use in pressure die-casting

A. Lousa^{a,*}, J. Romero^a, E. Martínez^a, J. Esteve^a, F. Montalà^b, L. Carreras^b

^a*Departament de Física Aplicada i Òptica, Universitat de Barcelona, Avda. Diagonal 647, E-08028 Barcelona, Catalunya, Spain*

^b*Tratamientos Térmicos Carreras, TTC S.A., C/Doctor Almera 85, E-08205 Sabadell, Catalunya, Spain*

Abstract

Chromium nitride coatings are known to give reasonable solutions to the requirements of semisolid forming tools and of pressure die-casting of low-melting-point metals and alloys. These hard coatings have good mechanical behavior when working at high temperatures. They show enhanced hardness and good wear and corrosion resistance, as well as reduced adhesion to the molten or semisolid metal. We have developed a related hard coating based on multilayered stacking of CrN and Cr metal layers with bilayer thickness down to 22 nm. This coating is obtained by both RF magnetron sputtering and reactive cathodic-arc physical vapor deposition (PVD) on hardened tool-steel substrates. Multilayered coatings are characterized with respect to their structure, hardness and adhesion, and compared for performance to standard CrN single-layer coatings. The Cr metal inter-layer and the multilayered film structure improve the adhesion of the coating to the steel substrate by reducing the stress and film brittleness, and by better matching of the thermal expansion coefficients. When the bilayer thickness was reduced, a reduction in residual stress, and an increase in hardness and critical load were observed. In particular, our Cr/CrN multilayers with a bilayer thickness less than 60 nm surpass all CrN single-film properties. © 2001 Elsevier Science B.V. All rights reserved.

Keywords: Multilayer; Chromium nitride; Reactive sputtering; Nanoindentation; Hard coatings

1. Introduction

Hard and corrosion-resistant coatings are frequently used to protect and enhance the lifetime of industrial components under high and constant wear loads. TiN is the standard among the transition metal nitride coatings employed in the industry, but requirements to withstand aggressive environments and to improve oxidation and wear resistance under extreme temperatures has led to chromium nitride [1,2]. Chromium coatings form a passivating oxide layer that does not allow further oxidation; explaining why chromium nitride is believed to be a promising solution to corrosive problems.

Recently, another approach to solve some coating problems has been to design new structures, such as multilayers. The multilayer concept has succeeded in a

broad range of applications, and is now being proposed as a promising way to improve the wear-resistance properties of hard coatings [3,4].

Since good results have been obtained using multilayer structures of Ti/TiN [4,5], the proposal of Cr/CrN multilayers as the next logical step is undoubtedly a path to future achievements. Even though these multilayer structures have not yet been extensively investigated, it has been recently reported [3,6] that the combination of hard but brittle CrN and tough but soft Cr in a multilayer structure enhances the wear resistance of each individual material. There is also a dependence of the multilayer properties on bilayer thickness.

In this paper, we present the results of a set of Cr/CrN multilayers deposited by RF magnetron sputtering under controlled ion bombardment during film growth. The multilayer period was varied from 100 to 20 nm in order to study the possible presence of multilayer effects in the film properties. Scanning electron microscopy (SEM) and secondary-ion mass spectrometry (SIMS)

* Corresponding author. Tel.: +34-93-402-1144; fax: +34-93-402-1138.

E-mail address: alousa@fao.ub.es (A. Lousa).

were used to confirm the multilayer structure. The dependence of the crystalline structure, stress, hardness and adhesion of the coatings on multilayer period are presented. These results are compared with those obtained on a set of cathodic arc-deposited coatings produced by TTC as commercial products.

2. Experimental

2.1. Materials

Chromium, chromium nitride and multilayered Cr/CrN thin films were deposited by both RF magnetron sputtering and cathodic arc deposition. Hardened steel (M-2, 1.3343), glass substrates and silicon wafers were used as substrates. Silicon and glass substrates were pre-cleaned in a hot acetone bath, rinsed ultrasonically in ethanol and de-ionized water and dried with dry nitrogen. Steel substrates ($1.5 \times 1 \text{ cm}^2$) were polished with 1- μm diamond powder, rinsed ultrasonically in ethanol and dried with dry nitrogen prior to loading into the deposition chamber.

2.2. Sputtering deposition

Sputtered films were deposited using a Cr (99.99% purity) disk target of 3 in. in diameter. Films were deposited at values of RF input power of 300 W. The substrate–target distance was kept at 5 cm. The substrate was heated by a quartz lamp to a substrate temperature of approximately 350°C. The base pressure in the chamber was $\leq 1 \times 10^{-4}$ Pa. Cr films were deposited in a pure Ar atmosphere at a pressure of 3.3×10^{-1} Pa. CrN films were deposited in a Ar (60%)/N₂ (40%) atmosphere at a pressure of 5.5×10^{-1} Pa. Two independent mass-flow controllers regulated both fluxes. The multilayered Cr/CrN structures were obtained by sequential RF magnetron sputtering. A programmable power supply was used to switch the N₂ flow between the values corresponding to the deposition of Cr and CrN.

In order to control the energy of bombarding ions during film growth, the substrate voltage was regulated by the ‘substrate tuning’ technique. A detailed description of the technique is given elsewhere [7]. Using this technique, simple and fine external control of the DC bias voltage developed at the anode (substrate) is achieved, from a positive value of some few 10s of V to a negative value slightly greater than 100 V, even for insulating materials. For the purpose of this work, the substrate voltage, V_{SO} , was fixed to -50 V (referenced to ground) in order to grow CrN films with satisfactory properties [8,9].

Before each deposition, pre-sputtering of the substrates was employed for more than 10 min in a pure argon atmosphere.

2.3. Cathodic arc deposition

Arc-deposited films were obtained in a multicathode arc evaporation system equipped with two Cr targets. The base pressure was lower than 2×10^{-3} Pa. The substrates were sputter cleaned and heated at a negative bias of 1200 V. The substrate temperature was 773 K, as measured with a calibrated pyrometer.

Simple Cr and CrN films were deposited at a pressure of 6×10^{-1} Pa using Ar and N₂ atmospheres, respectively. The negative substrate bias during film deposition was -150 V. Multilayer structures were obtained by alternatively changing the gas composition.

2.4. Coatings characterization

Film thickness measurements were performed using a profilometer and compared with scanning electron micrographs results. Lamellar thickness was measured by SEM (when possible) and SIMS. Film composition was studied by XPS and SIMS analysis. SIMS analysis was performed using oxygen ions at 9 keV and 400 nA, except for the thinnest lamellar multilayer, for which 4.5 keV and 300 nA were used in order to improve depth resolution.

X-Ray diffraction analysis was performed to identify the crystallographic structure and preferred orientations of the coatings.

The stress-induced curvature was measured by a surface profiler. Stresses were calculated from these values using Stoney’s equation. Hardness, Young’s modulus and elastic recovery were characterized by dynamical nanoindentation (NanoTest 550, Micro Materials Ltd) with a Berkovich diamond tip. The hardness and Young’s modulus values were obtained by the Oliver and Pharr analysis method [10]. In order to avoid substrate effects, the indenter penetration depths were limited to maximum depths of 15% of the coating thickness.

The adhesion of films to the steel substrate was evaluated by the microscratch technique using a spherical diamond indenter of 50 μm in radius. The scratches were produced by increasing the load up to a maximum of 12 000 mN. The failure mechanisms and corresponding critical load values have been established from SEM scratch images.

3. Results and discussion

3.1. Composition and structure of Cr and CrN sputtered films

Films of simple Cr and CrN were deposited in the first place in order to check the quality of the materials. The deposition rates of both coatings were used to determine the deposition times needed to grow the

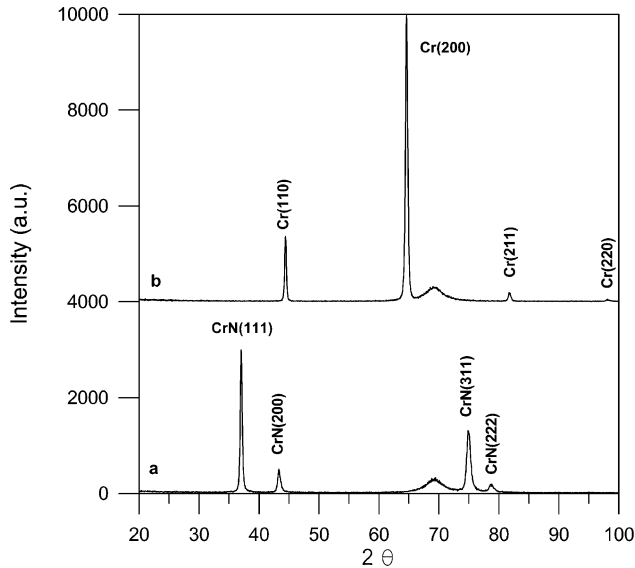


Fig. 1. Diffraction patterns of sputtered films: (a) CrN; and (b) Cr.

desired multilayer structures. Under our experimental conditions, the deposition rates of both Cr and CrN films were very similar, near $1.4 \mu\text{m}/\text{h}$.

Compositional XPS analysis on a single chromium nitride layer reveals an almost stoichiometric 1:1 CrN composition. A similar result was reported for films deposited under similar conditions [8,9,11]. SIMS compositional depth profile analysis indicates a constant composition over all of the film.

X-Ray diffraction analyses of the simple films are shown in Fig. 1. Chromium nitride single film (Fig. 1a) presents a pattern clearly identified as cubic CrN, with strong (111) and (311) peaks, and less intense (200) and (222) ones [12]. There were no signals observed that reveal the presence of Cr_2N . Cr film (Fig. 1b) shows diffraction peaks with a strong (200) reflection, an important (110) and weak (211) and (220) reflections. The relative intensity I_{200}/I_{110} in our Cr film is approximately 27-fold higher than that of the powder diagram (JCPDS 06-0694), in which (110) is the most intense peak. Thus, a strong (200) preferred orientation parallel to the sample surface could be deduced.

3.2. Composition and structure of Cr/CrN sputtered multilayers

Four multilayers were deposited for 1 h, having thickness values close to $1.4 \mu\text{m}$, with different thickness of the individual layers and a Cr/CrN ratio close to 1:1. All multilayers were produced following the same sequence, with a Cr layer as the innermost one and a chromium nitride layer as the outermost one, varying the number of lamellae from 12 to 60, including 20 and 30. Thus, approximate lamellae thickness values are 110, 70, 45 and 22 nm.

SEM images (Fig. 2a) confirmed the expected well-defined and uniform multilayer structure of those coatings, with approximately the same Cr and CrN thickness in the bilayer. SEM images showed the designed lamellar thickness, except for the thinnest one, which could not be clearly resolved by this technique.

SIMS analyses showed a clear modulated composition consistent with the Cr/CrN multilayer structure for all the multilayers. Fig. 3 shows the SIMS analysis of the 45-nm lamellar multilayer. The chromium signal is nearly constant, except for small oscillations due to a matrix effect, while the nitrogen signal shows a periodic oscillation that is clearly due to a multilayer Cr/CrN structure. The reduction in the difference between maxima and minima can be explained as a progressive effect of ion implantation as SIMS analysis progresses. The nitrogen signal ($^{14}\text{N}^+$) quickly diminishes to very low values when the silicon substrate is reached, after a correction for the contribution of $^{28}\text{Si}^{2+}$ was carried out.

Fig. 4 shows details of the SIMS nitrogen-signal dependence on depth, corresponding to the four multilayers. The temporal dependence of the experimental SIMS results has been transformed to spatial dependence via profilometer measurements in the resulting SIMS crater. For the thickest lamellar multilayer, it is evident that the modulation in $^{14}\text{N}^+$ signal is greater than two orders of magnitude and the maximum signal almost reaches the value obtained in simple CrN films. For the other multilayers, a clear modulation in $^{14}\text{N}^+$ signal is also observed, although the modulation amplitude is progressively reduced as the bilayer thickness is reduced. Bearing in mind the good multilayer structure observed by SEM, this effect can only be attributed to intrinsic limitations in depth resolution associated to the SIMS technique. Thus, the thinner the bilayer, the greater the loss of contrast.

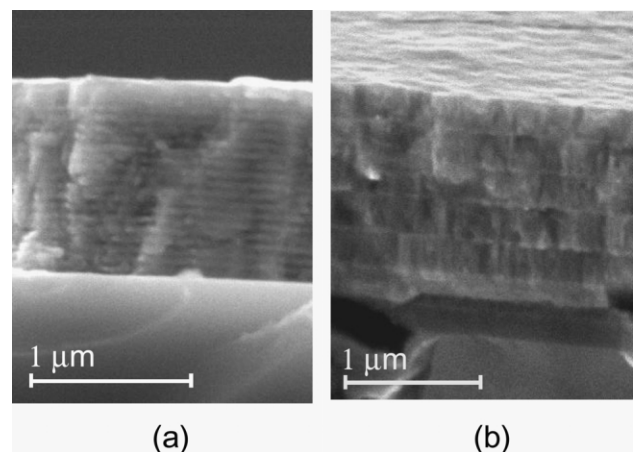


Fig. 2. SEM images of: (a) a sputtered 20-bilayer Cr/CrN multilayer; and (b) a cathodic arc-deposited 6-bilayer Cr/CrN multilayer.

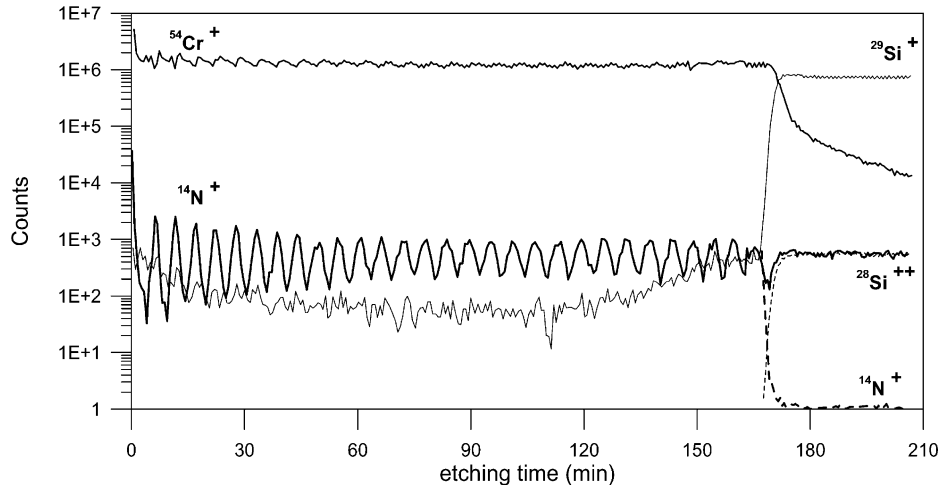


Fig. 3. SIMS analysis of a 30-bilayer Cr/CrN multilayer.

Multilayer diffraction patterns are shown in Fig. 5. All multilayers have a characteristic diffraction pattern, where the only important observed reflections for Cr and CrN are (200) peaks in both cases. Only weak (311) and (400) CrN reflections in all multilayer diffractograms and a very weak (111) reflection in the thickest lamellar multilayer pattern are observed. These results show that the crystalline orientation of the Cr and CrN layers in a Cr/CrN multilayer is very different from that observed in simple Cr and CrN films (Fig. 1). The (111) preferred orientation observed in simple CrN films of 1.4 μm , has now turned into a clear (200) orientation. Mutual influences between the Cr and CrN structures when they grow together in very thin layers provide a natural explanation for these results.

3.3. Composition and structure of CrN and multilayers in cathodic arc-deposited films

Simple CrN films and a set of Cr/CrN multilayer structures were deposited by cathodic arc deposition on hardened steel with a thickness of approximately 1.5 mm. The compositional XPS analysis on the single chromium nitride layer indicates a nearly stoichiometric 1:1 CrN composition.

Fig. 2b shows a SEM image of a Cr/CrN multilayer formed by 6 bilayers of approximately 240-nm bilayer thickness. It is evident that the thickness of the Cr monolayer is thinner (approx. one tenth) than the CrN monolayer thickness.

SIMS analysis indicates a constant depth composition over all of the CrN film. The multilayer structure was difficult to observe due to the low value (>2 nm) of the Cr layer thickness, but it was clearly observed when using low ion energy (4.5 keV).

X-Ray diffraction analyses of a simple CrN film and a Cr/CrN multilayer are shown in Fig. 6. The chromium

nitride single layer (Fig. 6b) presents a pattern clearly identified as cubic CrN, with a strong (111) peak, and less intense (200), (311), (222) and (211) peaks. As in the case of sputtered multilayers discussed above, the (111) preferred orientation observed in simple CrN films

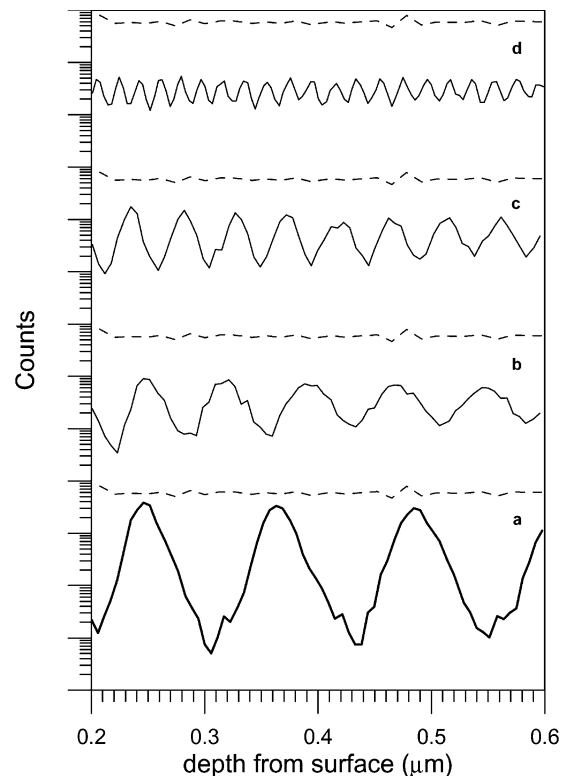


Fig. 4. SIMS depth profile detail of $^{14}\text{N}^+$ signal of Cr/CrN sputtered multilayers with different bilayer thickness: (a) 55/55; (b) 35/35; (c) 22/22; and (d) 11/11 nm. Dotted lines indicate $^{14}\text{N}^+$ signal in single CrN film.

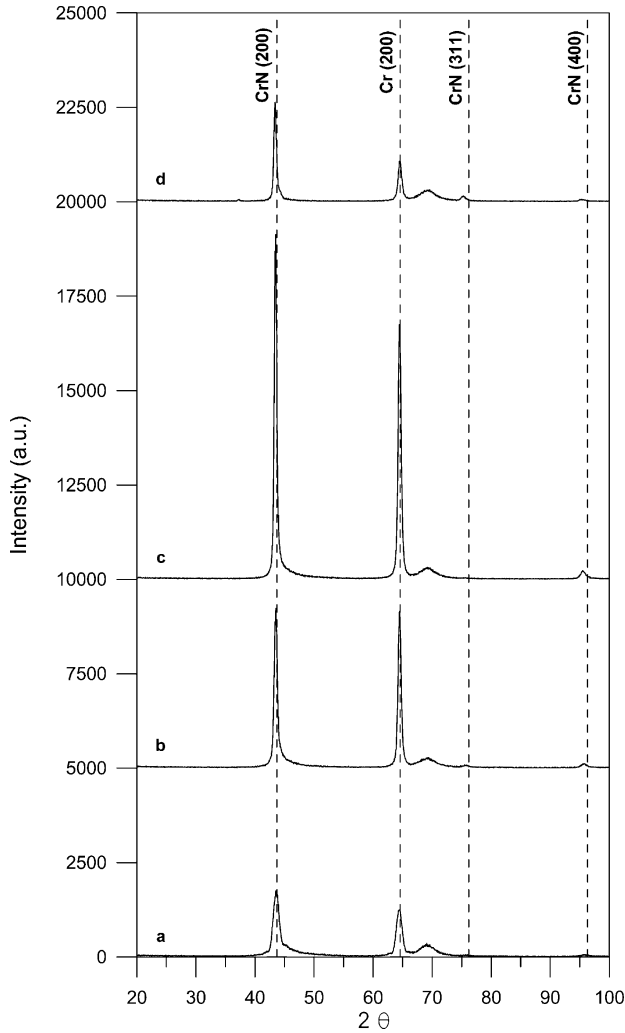


Fig. 5. Diffraction patterns of Cr/CrN sputtered multilayers with different bilayer thickness: (a) 11/11; (b) 22/22; (c) 35/35; and (d) 55/55 nm.

of 1.4 μm , has now turned into a clear (200) orientation, but in this case the most important Cr peak is (110).

3.4. Mechanical properties

Residual stress in the sputtered films was detected by measuring the stress-induced curvature on films deposited on 0.3-mm-thick silicon wafers. Using Stoney's equation, the compressive stress was 1.4 and 2.8 GPa in the Cr and CrN films, respectively. Stress in all multilayers is lower than in CrN, decreasing from 1.7 to 0.53 GPa as the bilayer thickness was reduced from 110 to 22 nm, as is evident in Fig. 7. This behavior is confirmed by a shift of the (200) peaks in the XRD diffraction patterns towards the powder diagram values as the bilayer thickness is decreased.

The hardness values for the CrN and Cr single layers were 18 and 7 GPa, respectively. Fig. 7 plots the

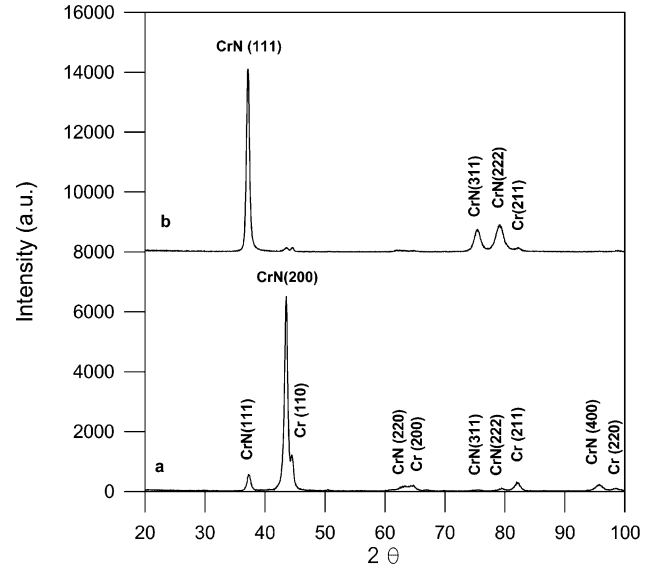


Fig. 6. Diffraction patterns of cathodic arc-deposited: (a) Cr/CrN multilayer; and (b) CrN single film.

hardness values measured for the CrN/Cr multilayer films obtained by RF magnetron sputtering as a function of the individual layer thickness (half of the modulation period). For greater layer thickness, the multilayer hardness values are between the Cr and CrN single-layer values. However, when the layer thickness is less than 30 nm, the multilayer hardness increases and surpasses the CrN single-layer value. These hardness values are consistent with those reported for CrN coatings obtained by the ion bombardment process [13], and also with values reported for CrN/TiN [14]. Measured Young's

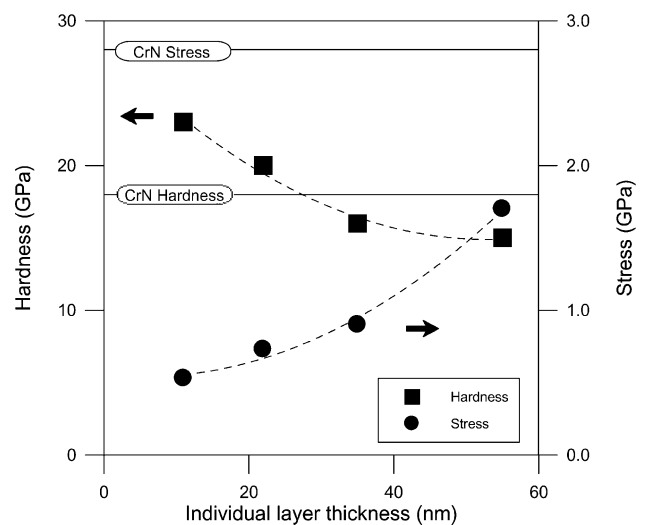


Fig. 7. Hardness and stress values as a function of the individual layer thickness (half of the modulation period) for the CrN/Cr multilayers deposited by RF magnetron sputtering. The hardness and stress values measured for the single-layer CrN are also plotted.

modulus values are between 250 and 310 GPa, the highest values corresponding to the thinner period multilayer. These values are similar to those found in the literature for similar coatings [15,16].

For the samples obtained by cathodic arc deposition, the hardness values of multilayers also surpassed that of the CrN single-layer coating, and the hardness increased when the multilayer thickness period decreased. In this series, the multilayer with the thinnest period consisted of 100-nm-thick CrN layers and 20-nm-thick Cr layers and showed a hardness of 22 GPa. This value is similar to those measured on the thinnest-period magnetron sputtering multilayers, despite the larger thickness period of cathodic arc multilayers. This can be attributed to the fact that, in this series, CrN is the thicker layer in the multilayer period.

Microscratch measurements showed that multilayers have excellent adherence to steel. The main failure mechanism observed for high loads is conformal cracking of the coating inside the scratch path. Only large-period multilayers showed adhesive failures outside the scratch path. The critical load values are between 3100 and 8000 mN; the largest value corresponds to the 20-nm individual-layer sample. The critical load increase for the thinnest period multilayers can probably be related to the reduction observed in internal stress for these coatings.

The reduced stress and increased adhesion on steel substrates found for the small-period Cr/CrN multilayers should improve the fair performance of the CrN coatings in pressure die-casting applications.

4. Conclusions

Well-defined Cr/CrN multilayers have been deposited by both RF magnetron sputtering and cathodic arc deposition with bilayer thickness down to 22 nm. The multilayer structure was confirmed by SEM and SIMS analysis. The multilayer structure induces a (200) pref-

erential growth of CrN layers. When the bilayer thickness was reduced, a reduction in residual stress, and an increase in hardness and critical load were observed. In particular, our Cr/CrN multilayers with a bilayer thickness below 60 nm surpass all CrN single-film properties

Acknowledgements

The authors acknowledge the Serveis Científico-Tècnics of the Universitat de Barcelona for XPS, XRD and SIMS measurements. This work has been supported by the C.I.C.Y.T. of Spain under contract MAT2000-1014-C02-02.

References

- [1] S.J. Bull, D.S. Rickerby, *Surf. Coat. Technol.* 43/44 (1990) 732.
- [2] Y.L. Su, S.H. Yao, Z.L. Leu, C.S. Wei, C.T. Wu, *Wear* 213 (1997) 165.
- [3] M. Berger, U. Wiklund, M. Eriksson, H. Engqvist, S. Jacobson, *Surf. Coat. Technol.* 116–119 (1999) 1138.
- [4] S.J. Bull, A.M. Jones, *Surf. Coat. Technol.* 78 (1996) 173.
- [5] U. Wiklund, P. Hedenqvist, S. Hogmark, *Surf. Coat. Technol.* 97 (1997) 773.
- [6] M.L. Kuruppu, G. Negrea, I.P. Ivanov, S.L. Rohde, *J. Vac. Sci. Technol. A* 16 (1998) 1949.
- [7] A. Lousa, S. Gimeno, *J. Vac. Sci. Technol. A* 15 (1997) 62.
- [8] X.-M. He, N. Baker, B.A. Kehler, K.C. Walter, M. Nastasi, *J. Vac. Sci. Technol. A* 18 (2000) 30.
- [9] L. Cunha, M. Andritschky, *Surf. Coat. Technol.* 111 (1999) 158.
- [10] W.C. Oliver, G.M. Pharr, *J. Mater. Res.* 7 (1992) 1564.
- [11] P. Hones, R. Sanjines, F. Lévy, *Surf. Coat. Technol.* 94/95 (1997) 398.
- [12] C. Meunier, S. Vives, G. Bertrand, *Surf. Coat. Technol.* 107 (1998) 149.
- [13] Y. Fu, X. Zhu, B. Tang et al., *Wear* 217 (1998) 159–166.
- [14] Y. Zhou, R. Asaki, W.H. Soe, R. Yamamoto, R. Chen, A. Iwabuchi, *Wear* 236 (1999) 159–164.
- [15] C. Gautier, H. Moussani, F. Elstner, J. Machet, *Surf. Coat. Technol.* 86/87 (1996) 254.
- [16] J.A. Sue, A.J. Perry, J. Vetter, *Surf. Coat. Technol.* 68 (1994) 126–130.